

X-ray Diffraction from a Helix of Any Length that Displays Cumulative Azimuthal Disorder

XIANG-QI MU,^a LEE MAKOWSKI^{b*} AND BEATRICE MAGDOFF FAIRCHILD^{a†}

^aHematology Division, Medical Service, St. Luke's-Roosevelt Hospital Center and Department of Medicine, College of Physicians and Surgeons of Columbia University, New York, NY 10025, USA, and ^bInstitute of Molecular Biophysics, Florida State University, Tallahassee, FL 32306-3015, USA. E-mail: makowski@sb.fsu.edu

(Received 21 June 1996; accepted 13 September 1996)

Abstract

An explicit formula has been derived to describe the attenuation and broadening of cylindrically averaged diffraction intensities from a helix of any given length which possesses cumulative azimuthal disorder. The application limits of an approximate formula, represented by the first term of this formula, are defined. Strategies to estimate the length of fibers, the degree of disorder, and the overlap of adjacent layer lines are outlined. Some features of diffraction patterns from the disordered helical structure of the HbS fiber are interpreted in light of these results. In these patterns, non-zero-order Bessel functions are attenuated and broadened due to azimuthal disorder and finite length. Adjacent layer lines overlap because of the very large axial repeat distance of the HbS fibers. As a result, the contribution of any Bessel function term with $n \geq 10$ is not discernible in these patterns. Only Bessel terms with $n < 6$ may be accurately estimated in these patterns, if instrumental broadening is negligible or correctable. The theory presented here may also be used to make a rough estimate of the degree of disorder in F-actin fibers by comparison of X-ray diffraction patterns with serial peak projections calculated assuming various degrees of disorder.

1. Introduction

The effect of cumulative azimuthal disorder on X-ray diffraction from a helix was first addressed by Egelman, Francis & DeRosier (1982) in their analysis of diffraction from F-actin. They suggested that in the X-ray diffraction patterns from oriented gels of F-actin, the intensity of layer lines was reduced by a factor proportional to n^2 , where n is the order of the dominant Bessel-function term contributing to the layer line. Egelman & DeRosier (1982) calculated the diffracted intensity from a cumulatively disordered helix by analogy with the calculation of the mean squared end-to-end distance in flexible polymers. From this analysis,

they derived an equation for the peak intensity of layer lines and showed that it is proportional to $1/n^2$. As the total intensity of X-ray scattering is a constant, the width of the layer line along the direction perpendicular to the layer line (Z direction) is proportional to n^2 . In this analysis, it was assumed that (i) the number of subunits in the structure was large, and (ii) the product of the degree of disorder and the order of the Bessel function was small.

This theory was extended by Barakat (1987), who obtained an equation for the peak intensity of layer lines from a cumulatively disordered helix based on rigorous statistical considerations. The only assumption in his analysis was that the random twists between subunits were uncorrelated Gaussian random variables with a zero mean and a small variance. Barakat's (1987) equations are applicable to disordered helices of any length, and for a sufficiently long helix they reduce to Egelman & DeRosier's (1982) results. For a sufficiently long helix with cumulative azimuthal disorder, the distribution of intensity along the Z direction has been derived by Inouye (1994) by comparison with the diffraction theory for one-dimensional paracrystalline disorder. These treatments do not, however, address all the properties of diffraction needed to completely characterize a helix of limited length that displays cumulative azimuthal disorder.

Sickle-cell hemoglobin (HbS) fibers have been shown to display cumulative azimuthal disorder (Carragher, Bluemke, Gabriel, Potel & Josephs, 1988; Lewis, Gross & Josephs, 1994). The number of subunits in a turn of the fiber has been observed to vary between 42 and 51 (Dykes, Crepeau & Edelstein, 1979; Carragher *et al.*, 1988), resulting in an average axial repeat of *ca* 3000 Å. Given the long axial repeat, even a small degree of disorder will result in layer lines broadening to the point that they overlap with adjacent layer lines. Quantitative estimation of this broadening cannot be made using previous treatments of azimuthal disorder since they assume a large number of subunits. The length of a typical HbS fiber may be as short as a few repeats (Briehl, Mann & Josephs, 1990).

[†] Dr Fairchild passed away on 23 August 1995.

In this paper, we present a rigorous derivation of the attenuated diffraction intensities and their broadening along the Z direction for an azimuthally disordered helix of limited length, and demonstrate the application of this theory to sickle-cell hemoglobin fibers.

2. Theory

We require the Fourier transform of a cylindrical structure consisting of N subunits on a cylindrical surface of radius r_0 , with a constant axial separation, p . For simplicity, the subunit is taken to be a point atom. This Fourier transform is

$$F(R, \Psi, Z) = \sum_{k=1}^N \exp\{2\pi i[Rr_0 \cos(\Psi - \varphi_k) + kpZ]\}, \quad (1)$$

where φ_k is the angular coordinate of the k th subunit. The intensity of diffraction from the structure is given by

$$I(R, \Psi, Z) = \sum_{k=1}^N \sum_{k'=1}^N \exp[2\pi i(k - k')pZ] \times \exp[2\pi iRr_0 \cos(\Psi - \varphi_k)] \times \exp[2\pi iRr_0 \cos(\pi - \Psi + \varphi_{k'})]. \quad (2)$$

Substitution into (2) of the following well known expansion (Watson, 1947)

$$\exp(iu \cos \theta) = \sum_{n=-\infty}^{+\infty} J_n(u) \exp[in(\theta + \pi/2)], \quad (3)$$

where $J_n(u)$ is the Bessel function of degree n , gives

$$I(R, \Psi, Z) = \sum_{k=1}^N \sum_{k'=1}^N \sum_{n=-\infty}^{\infty} \sum_{n'=-\infty}^{\infty} \exp[2\pi i(k - k')pZ] \times J_n(2\pi Rr_0) J_{n'}(2\pi Rr_0) \times \exp[i(n - n')(\Psi + \pi/2)] \times \exp[-i(n\varphi_k - n'\varphi_{k'})]. \quad (4)$$

The cylindrically averaged intensity over the angle Ψ of a bundle of parallel, non-interfering, similar structures is

$$I(R, Z) = \sum_{k=1}^N \sum_{k'=1}^N \sum_{n=-\infty}^{\infty} \exp[2\pi i(k - k')pZ] J_n^2(2\pi Rr_0) \times \exp[-in(\varphi_k - \varphi_{k'})] \quad (5)$$

as shown by Franklin & Klug (1955) for a regular helix. We rewrite (5) as

$$I(R, Z) = \sum_{n=-\infty}^{\infty} J_n^2(2\pi Rr_0) W(n, Z), \quad (6)$$

where

$$W(n, Z) = \sum_{k=1}^N \sum_{k'=1}^N \exp[2\pi i(k - k')pZ] \times \exp[-in(\varphi_k - \varphi_{k'})]. \quad (7)$$

For a regular helix with u/v symmetry where there are u subunits in v turns in the axial repeat, $c (= up)$, and where $\varphi_k = k(2\pi v/u)$, the equation becomes

$$W(n, Z) = \sum_{k=1}^N \sum_{k'=1}^N \exp[2\pi i(k - k')(pZ - nv/u)]. \quad (8)$$

The value of the function $W(n, Z)$ is equal to zero except at the discrete points defined by

$$pZ - nv/u = m, \quad m = 0, \pm 1, \pm 2, \pm 3, \dots, \quad (9)$$

at which points $W(n, Z) = N^2$. From this equation, we find that $Z = (um + vn)/up$, where $up = c$, the helical repeat, and $um + vn = l$, another integer. The function $W(n, Z)$ is therefore an expression of the selection rule from the classical theory of helical diffraction (Cochran, Crick & Vand, 1952). For a non-regular helix, the function $W(n, Z)$, rather than being a discrete set of points along Z , is usually continuous along the Z direction.

For a helix displaying cumulatively azimuthal disorder, where the disorder is not 'too large', an 'average helix', with a symmetry of u/v , may exist over a limited range. The angular coordinate of its k th subunit may be written as (Egelman & DeRosier, 1982; with a different symbol and a different unit for g_j):

$$\varphi_k = k(2\pi v/u) + \sum_{j=1}^k 2\pi g_j, \quad (10)$$

where g_j is an uncorrelated random Gaussian variable with zero mean. The standard deviation of the variable g_j , $\langle g_j^2 \rangle^{1/2}$, denoted by g , is a measure of the degree of disorder of the system.

Substitution of (10) into (7) gives

$$W(n, Z) = \sum_{k=1}^N \sum_{k'=1}^N \exp[2\pi i(k - k')(pZ - vn/u)] \times \exp \left[-in \left(\sum_{j=1}^k 2\pi g_j - \sum_{j=1}^{k'} 2\pi g_j \right) \right]. \quad (11)$$

As pointed out by Barakat (1987), the ensemble averaging over g_j for the second exponential can be expressed in terms of g . $W(n, Z)$, averaged over all values of g_j , after replacement of the double summation by a single one as usual (Vainstein, 1966), becomes

$$\langle W(n, Z) \rangle = N + 2 \sum_{k=1}^{N-1} (N - k) \cos[2\pi k(pZ - vn/u)] \times \exp(-2\pi^2 n^2 k g^2). \quad (12)$$

This averaged $\langle W(n, Z) \rangle$ describes the broadening of a Bessel-function term of order n due to azimuthal

disorder with standard deviation, g , in a helix of N subunits.

For convenience, two new variables are introduced:

$$\alpha = 2\pi(pZ - nv/u), \quad (13)$$

$$\beta = \exp(-2\pi^2 n^2 g^2). \quad (14)$$

The function $\langle W(n, Z) \rangle$ may then be written as

$$\langle W(n, \alpha) \rangle = N + 2 \sum_{k=1}^{N-1} (N-k) \beta^k \cos k\alpha. \quad (15)$$

The explicit form for the first sum in (15) is taken from Gradshteyn & Ryzhik (1980):

$$\begin{aligned} \sum_{k=1}^{N-1} \beta^k \cos k\alpha &= [\beta \cos \alpha - \beta^2 - \beta^N \cos N\alpha \\ &+ \beta^{N+1} \cos(N-1)\alpha] \\ &\times (1 - 2\beta \cos \alpha + \beta^2)^{-1}, \end{aligned} \quad (16)$$

and the second sum is the derivative of the first with respect to β .

Equation (15), after summation according to the above, becomes

$$\begin{aligned} \langle W(n, \alpha) \rangle &= N(1 - \beta^2)/(1 - 2\beta \cos \alpha + \beta^2) \\ &- 2\beta(\cos \alpha - 2\beta + \beta^2 \cos \alpha) \\ &\times (1 - 2\beta \cos \alpha + \beta^2)^{-2} \\ &+ 2\beta^{N+1}[\cos(N+1)\alpha - 2\beta \cos N\alpha \\ &+ \beta^2 \cos(N-1)\alpha] \\ &\times (1 - 2\beta \cos \alpha + \beta^2)^{-2}. \end{aligned} \quad (17)$$

Henceforth, the above function will be referred to as the broadening function of the Bessel term J_n^2 . In combination with the appropriate Bessel functions, (6) combined with (17) describes the scattered intensity in reciprocal space of a cumulatively disordered helix of any length.

The profile along the Z direction, the height and width of $\langle W(n, \alpha) \rangle$ or $\langle W(n, Z) \rangle$, depend on two factors: (i) the helix length, or the total number of subunits, N , in the structure, and (ii) the degree of disorder of the structure, g .

The principal maxima of the broadening function occurs at α equal to zero or an integer multiple of 2π , and (17) becomes

$$\begin{aligned} \langle W(n, 0) \rangle &= N(1 + \beta)/(1 - \beta) - 2\beta/(1 - \beta)^2 \\ &+ 2\beta^{N+1}/(1 - \beta)^2. \end{aligned} \quad (18)$$

This equation corresponds to equation (3.2) obtained by Barakat (1987) through statistical considerations.

To examine the broadening function for the zero-order Bessel function, n is placed equal to zero in (12) and $\alpha = 2\pi pZ$. The broadening function then becomes

$$W(0, \alpha) = N + 2 \sum_{k=1}^{N-1} (N-k) \cos k\alpha, \quad (19)$$

which, upon summation, gives

$$W(0, \alpha) = \sin^2(N\alpha/2)/\sin^2(\alpha/2). \quad (20)$$

When α is zero, $W(0, 0) = N^2$. The broadening function, (17), normalized by $W(0, 0)$ becomes

$$\begin{aligned} \langle w(n, \alpha) \rangle &= (1/N)(1 - \beta^2)/(1 - 2\beta \cos \alpha + \beta^2) \\ &- (1/N^2)2\beta(\cos \alpha - 2\beta + \beta^2 \cos \alpha) \\ &\times (1 - 2\beta \cos \alpha + \beta^2)^{-2} \\ &+ (1/N^2)2\beta^{N+1}[\cos(N+1)\alpha \\ &- 2\beta \cos N\alpha + \beta^2 \cos(N-1)\alpha] \\ &\times (1 - 2\beta \cos \alpha + \beta^2)^{-2}, \end{aligned} \quad (21)$$

which will be used to examine the effect of changes in g and N .

The maxima of the normalized broadening function are

$$\begin{aligned} \langle w(n, 0) \rangle &= (1/N)(1 + \beta)/(1 - \beta) - (1/N^2)2\beta/(1 - \beta)^2 \\ &+ (1/N^2)2\beta^{N+1}/(1 - \beta)^2 \end{aligned} \quad (22)$$

and, for $n = 0$,

$$w(0, 0) = 1. \quad (23)$$

To examine the properties of the broadening function, $\langle w(n, \alpha) \rangle$ as a function of α is plotted for various helical lengths and degrees of cumulative disorder in Fig. 1. For zero-order Bessel terms, neither the height nor the width of $w(0, \alpha)$ are affected by the degree of cumulative disorder, as shown by the bold curves in Figs. 1(c),(d),(e), where the disorder increases successively for equal numbers of subunits. When g remains constant, the width of $w(0, \alpha)$ decreases with increasing numbers of subunits, N , as seen in Figs. 1(a),(b),(c).

By contrast, non-zero-order Bessel terms are markedly affected by both azimuthal disorder and the length of the helix. The maxima of non-zero-order Bessel terms decrease with increasing Bessel order n , with increasing degree of disorder g (light lines in Figs. 1c,d,e), and with increasing numbers of subunits N , as shown in Figs. 1(a),(b),(c). The widths of the maxima increase with increasing Bessel orders, increasing degree of disorder, g , and as the number of subunits, n , decreases.

The contribution of each of the terms of (21) is shown in Fig. 2 for a disordered helix with $(ng) = 5.4/360$. Plots are shown for values of N equal to (a) 200, (b) 400, (c) 600, (d) 800, and (e) 2000. The thin continuous line, the broken and the dotted lines represent the three terms of (21), respectively. The thick line is the summation of all of these terms, or the broadening

function $\langle w(n, \alpha) \rangle$. For non-zero-order Bessel terms, all of the terms from (21) decrease with increasing N . The third term goes to zero for a moderately long helix, and both the second and the third terms may be ignored for a sufficiently long helix. In that case, the function $\langle w(n, \alpha) \rangle$ may be approximated by the first term:

$$\langle w(n, \alpha) \rangle = (1/N)(1 - \beta^2)/(1 - 2\beta \cos \alpha + \beta^2). \quad (24)$$

This equation corresponds to equation (10) of Inouye (1994) derived assuming a large number of subunits.

As shown in Fig. 2, when N is sufficiently large, the peak value and the profile of the function obtained from the approximate equation (24) approaches that obtained from the exact equation (21). Let us define a 'sufficient' length of a disordered fiber as the lower limit of length where the approximate formula (24) is applicable. Then, a 'sufficient' length consisting of a 'sufficiently' large number of subunits may be defined for any

required accuracy. For example, a requirement of 95% accuracy demands that N be at least $N_{\text{sup}}^{0.95}$, where $N_{\text{sup}}^{0.95}$ is the value of N at which the ratio of $\langle w(1, 0) \rangle$ from the exact equation (21) to that from the approximate equation (24) is not less than 95%. This may be derived from comparison of the calculations for the first-order Bessel-function terms, since they have the largest value of non-zero terms and the largest value of the broadening function.

It can be shown from (21) that if a disordered helix is infinitely long the broadening function $\langle w(n, \alpha) \rangle$ will be equal to zero for any non-zero Bessel-function term.

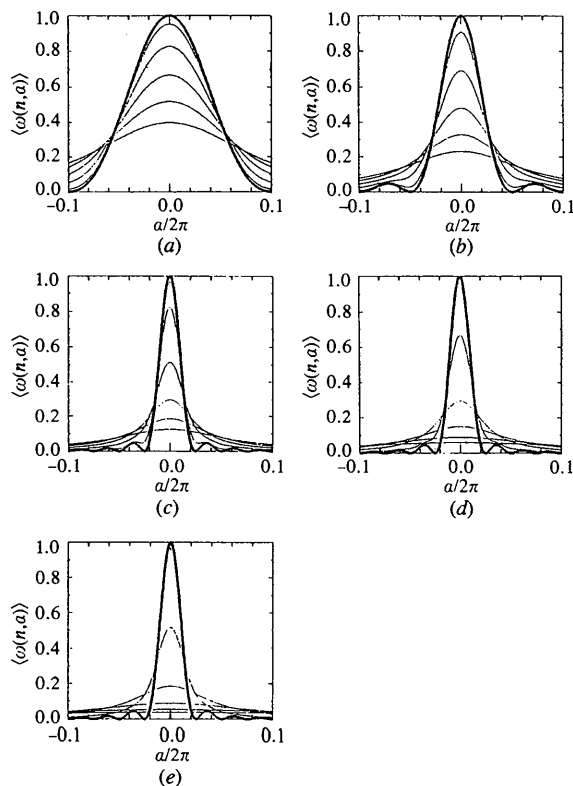


Fig. 1. Curves of $\langle w(n, \alpha) \rangle$ plotted against $a/2\pi$, in the range -0.1 to 0.1 , for (a) $N = 10$, $g = 10/360$; (b) $N = 20$, $g = 10/360$; (c) $N = 40$, $g = 10/360$; (d) $N = 40$, $g = 15/360$; (e) $N = 40$, $g = 20/360$. The thick lines are for $n = 0$, the thin lines are for $n = 1, 2, 3, 4$ and 5 , progressively down from $n = 0$. Both maximum and width of $w(n, \alpha)$ decrease with increasing N for non-zero Bessel terms, while the maximum decreases and the width increases with increasing g and with increasing n . The maximum of $w(0, \alpha)$ is always equal to 1.0, while its width is g -independent and decreases with increasing N .

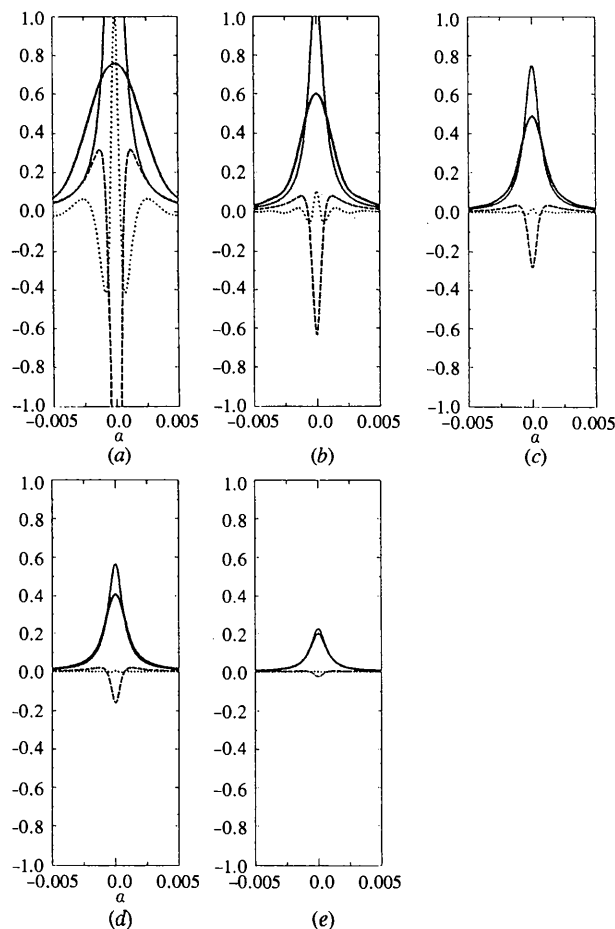


Fig. 2. The normalized broadening function $\langle w(n, \alpha) \rangle$ and its three constituent terms as written in formula (21), plotted for a disordered helix with $(ng) = 5.4/360$ and (a) $N = 200$; (b) $N = 400$; (c) $N = 600$; (d) $N = 800$; (e) $N = 2000$. The thick lines represent the broadening function, the thin solid, broken and dotted lines represent its three terms, respectively. All of the terms and the function itself decrease with increasing N . The third term can be ignored at $ca N = 600$, as shown in (c) where the broadening function may be represented by two terms of equation (21). Both the second and the third terms may be ignored at much larger values of N [e.g. 2000 as shown in (e)], where the approximate formula, (24), becomes valid.

$w(0, \alpha)$, the broadening function for the zero Bessel-function term, however, always has the value of 1.0 at $\alpha = 0$. Its width decreases with increasing N . The diffraction pattern from this system will then consist of a series of sharp layer lines with spacing of $1/p$.

There are two forms of the broadening function, *i.e.* $\langle w(n, \alpha) \rangle$ and $\langle w(n, Z) \rangle$. In the first form, all of the functions $\langle w(n, \alpha) \rangle$, with various Bessel orders, are placed at a common origin, corresponding to the common peak position. This allows the investigation of the effects of fiber length and degree of the disorder on the function, as shown above. To survey the effects of the degree of disorder and the fiber length on the whole diffraction pattern, the function $\langle w(n, Z) \rangle$ must be examined. A change in variable from α to Z according to (13) effects the change from $\langle w(n, \alpha) \rangle$ to $\langle w(n, Z) \rangle$. The peak positions of $\langle w(n, Z) \rangle$ depend on the symmetry of the fiber and Bessel order, and are spread along the Z direction in reciprocal space.

For example, by changing the origins of the curves in Fig. 1(c) according to (13), imposing a helical symmetry of $2/5$, and expanding n from -10 to $+10$, we have the broadening function $\langle w(n, Z) \rangle$ over a complete period in the range from 0 to $1/p$, as shown in Fig. 3. The positions of maxima of the curves for each n value are identical with those predicted by the selection rule for a regular helix of the same symmetry, and are marked below each peak. The functions $\langle w(n, Z) \rangle$ with low Bessel orders are sharper, while those with higher order are broader and prone to overlap with neighbors. The interval between adjacent layer lines depends on the value of u , the number of subunits in a long period of the structure. If u is very large, the layer lines may overlap even if the degree of disorder is small.

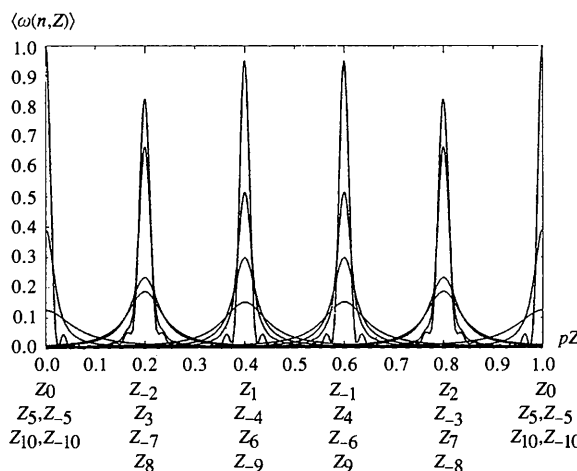


Fig. 3. Curves of the broadening function $\langle w(n, Z) \rangle$ versus Z , $n = -10$ to 10, for a disordered helix with $N = 40$, $g = 5/360$ and symmetry of $5/2$. They were obtained by moving the origins of $\langle w(n, \alpha) \rangle$ according to formula (13). The positions of maxima are marked as Z_n , where $n = -10$ to 10.

3. Applications

3.1. Measurement of N and g

Generally speaking, it is difficult to measure the averaged fiber length and the degree of disorder from the broadening of layer lines for a helix with cumulative angular disorder. This is true because the layer-line intensity is a summation over several Bessel terms, each attenuated by different degrees and broadened along the Z direction to varying extent.

When a single Bessel term makes a dominant contribution to a layer-line intensity, the fiber length can be estimated from the zero-order Bessel broadening, and the degree of disorder measured from non-zero Bessel terms. From (20), it is possible to derive a formula that relates the number of subunits, N , with ΔZ , the width at half-maximum of the broadening function curve $w(0, Z)$:

$$N = 0.89/p\Delta Z. \quad (25)$$

This equation is formally the same as Scherrer's equation for measuring crystallite size (Scherrer, 1918). It is not difficult to obtain the degree of disorder for a sufficiently long fiber. The width at half-maximum of function $\langle w(n, \alpha) \rangle$ in the approximate equation (24) is

$$\Delta\alpha = 2 \arccos[1 - (1 - \beta)^2/2\beta], \quad (26)$$

where $\Delta\alpha$ is twice the value of α , at which point the function $\langle w(n, \alpha) \rangle$ is half-maximum. Obviously, $\Delta\alpha$ depends on both n and g . In fact, the factors n and g always appear together, as shown in (14). For convenience, n and g can be considered as a single parameter. When the product (ng) is small, $\Delta\alpha$ may be approximated as

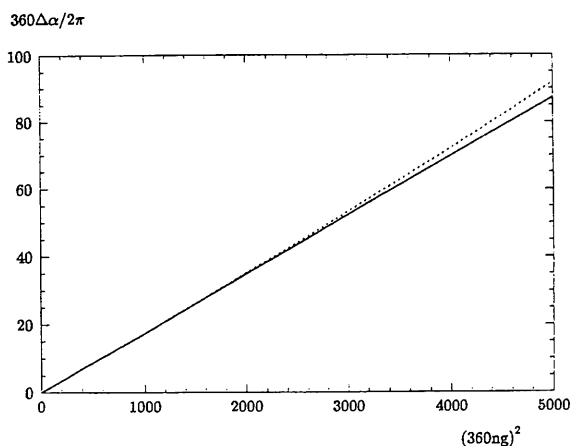


Fig. 4. Curves of the width of the broadening function, $\Delta\alpha$, versus the degree of disorder, $(ng)^2$, for a sufficiently long fiber. The discontinuous line and the continuous one were obtained by using formulae (26) and (27), respectively. $\Delta\alpha$ very quickly increases with increasing (ng) , but is N -independent. For smaller values of (ng) , formula (27) is a good approximation of (26). It underestimates $\Delta\alpha$ by only $\sim 5\%$ even when (ng) is as large as $70/360$.

$$\Delta\alpha = 4\pi^2(ng)^2. \quad (27)$$

Plots of $\Delta\alpha$ versus (ng) are shown in Fig. 4, where the continuous and dotted curves are obtained by the use of (28) and (29), respectively. The difference between the two curves can be ignored completely when (ng) is less than 50/360. The difference remains less than 5% even for a value of (ng) as high as 70/360. For a sufficiently long fiber, the maximum of function $\langle w(n, \alpha) \rangle$ is inversely proportional to N , but its width is independent of N .

When the fibers are short, (27) is no longer valid, while (25) is still applicable to estimate the fiber length. Substitution of N , obtained from (25), and an assumed value for degree of disorder into (21) gives a calculated broadening function. By minimizing the discrepancy between the latter and observed broadening, accurate values for both fiber length and degree of disorder can then be obtained based on the principle of least squares.

3.2. HbS fiber

The HbS fiber is a helical structure with subunit twist of $\sim 8^\circ$, or axial period of $\sim 3000 \text{ \AA}$ (Dykes, Crepeau & Edelstein, 1979; Carragher *et al.*, 1988). X-ray diffraction patterns from HbS fibers, however, display only layer lines with spacings of $1/64 \text{ \AA}^{-1}$, and lack the major features expected in diffraction from a helical structure (Fairchild & Chiu, 1979). The discovery of cumulative azimuthal disorder in this fiber (Carragher *et al.*, 1988; Lewis, Gross & Josephs, 1994) and the theory developed here make it possible to explain these observations and to estimate the effects of limited length and disorder on the pattern.

Two methods based on the above theory may be used to estimate the overlap of adjacent layer lines in diffraction patterns from HbS fibers.

(a) *The ratio of background to peak for a broadening function.* Define the ratio of background to peak intensity as

$$B/P = \frac{\langle w(n, Z_n + 0.5/up) \rangle}{\langle w(n, Z_n) \rangle}, \quad (28)$$

where Z_n is the peak position of $\langle w(n, Z) \rangle$ and $(Z_n + 0.5/up)$ is its background position, halfway between adjacent layer lines. Consider a function $\langle w(n, Z) \rangle$ with $B/P < 0.2$ as well separated from its neighbors, and any broadening function with $B/P > 0.2$ as exhibiting significant overlap. If the B/P ratio is larger than 0.8, the function $\langle w(n, Z) \rangle$ will not show a peak in any sense, being a relatively flat function with a width greater than the layer-line spacing. In other words, a Bessel term broadened by this function will contribute equally to observed layer lines and apparent background. The curves of B/P for HbS fibers, with $u = 48$, for values of N equal to 20, 40, 60, 100, 500 and 9000, are plotted against (ng) in Fig. 5. As expected, the ratio increases with increasing degree of

disorder, with increasing Bessel order, and with decreasing fiber length. The curve for $N = 500$ is not significantly different from that of longer fibers and may be regarded as the smallest values of B/P for a helical structure with symmetry of 48/1. It intersects with the lines $B/P = 0.2$ and $B/P = 0.8$ at $(ng) = 14/360$ and $(ng) = 29/360$, respectively. The value of g estimated from electron micrographs of HbS fiber is $2.7/360$ (Carragher *et al.*, 1988). Given this estimate, in the HbS fiber diffraction pattern, any Bessel term with $n > 10$ will be flattened completely, and only Bessel terms with $n < 6$ are, in principle, capable of being observed and estimated. For shorter fibers, these effects are even more serious.

(b) *Peak projection along the R direction of the diffraction intensity.* The peak projection for a disorder helix with point-atom subunits is defined as

$$i(Z) = \sum_{n=-\infty}^{+\infty} j_n^2(w(n, Z)), \quad (29)$$

where j_n^2 is the principal maximum of $J_n^2(2\pi Rr_0)$. This corresponds to a projection of diffraction intensities along the direction parallel to the layer lines. The projections for the HbS fiber with $u = 48$, $g = 2.7/360$ and $N = 24, 96$ and 192 are shown in Figs. 6(a),(b),(c). The conclusion from this figure is identical with that from the curves of B/P : only Bessel terms with $n < 6$ will be observable in the X-ray diffraction pattern of an HbS fiber. More Bessel terms become detectable as the degree of disorder is reduced, as shown in Figs. 6(d),(e),(f).

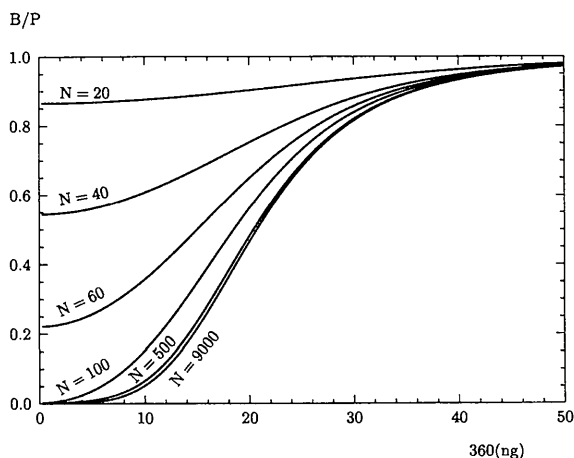


Fig. 5. Curves of the ratio of background (halfway between layer lines) to peak height, B/P , against the degree of disorder, (ng) , for a fiber with $u = 48$ and various values of N . Bessel-function terms for which $B/P < 5\%$ may be separated from neighboring layer lines very well. A Bessel-function term with $B/P > 80\%$ is essentially flat. For HbS fibers, where $u = 48$ and $g = 2.7/360$, any term with $n > 10$ is indistinguishable from noise, and only those terms with $n < 6$ may be measurable.

3.3. F-Actin fiber

The F-actin fiber was the first helical structure demonstrated to exhibit cumulative azimuthal disorder (Egelman, Francis & DeRosier, 1982; Egelman & DeRosier, 1982; Egelman, 1992). The helical symmetry of the fiber is 13/6. Various values for the degree of disorder, from 5° through 15° , were reported, as summarized in Egelman's review article (Egelman, 1992). The degree of disorder and fiber length can be measured quantitatively on a high-quality diffraction pattern from an F-actin sample (Popp, Lednev & Jahn, 1987; Holmes, Popp, Gebhard & Kabsch, 1990) using the method mentioned in §3.1. A semi-quantitative estimate of the degree of disorder of F-actin fibers may be made as follows. Peak projections for F-actin calculated from values of g as 0, 3, 6, 9, 12 and 15° are plotted in Fig. 7. When $g \leq 3^\circ$, every layer line will appear in the pattern, with only minor overlapping. However, higher-order Bessel terms gradually disappear with increasing disorder, as shown in Figs. 7(a)–(f). The sixth and seventh layer lines, constituted largely of a first-order Bessel term, are still very clear even for g as high as 15° , but other layer lines almost

disappear for this degree of disorder. Visual comparison of these results with diffraction patterns from F-actin indicates that the degree of disorder in the F-actin fibers is usually larger than 9° .

4. Discussion

Two approaches to the analysis of X-ray diffraction from helices with cumulative angular disorder have been pursued. The first approach (Egelman & DeRosier, 1982; Barakat, 1987; Inouye, 1994; present paper) is to decompose the diffracted intensity into its Bessel terms and calculate each term by the contributions from each subunit pair of the helix. The second approach (Worthington & Elliott, 1989) is very different in that the diffracted intensity is calculated directly from the contributions of each subunit pair. Analytically, it is impossible to compare the equations resulting from the first approach with those from the second, but the final numerical results, obtained from similar models, should be comparable. The advantage of the first kind of approach is obvious; an explicit

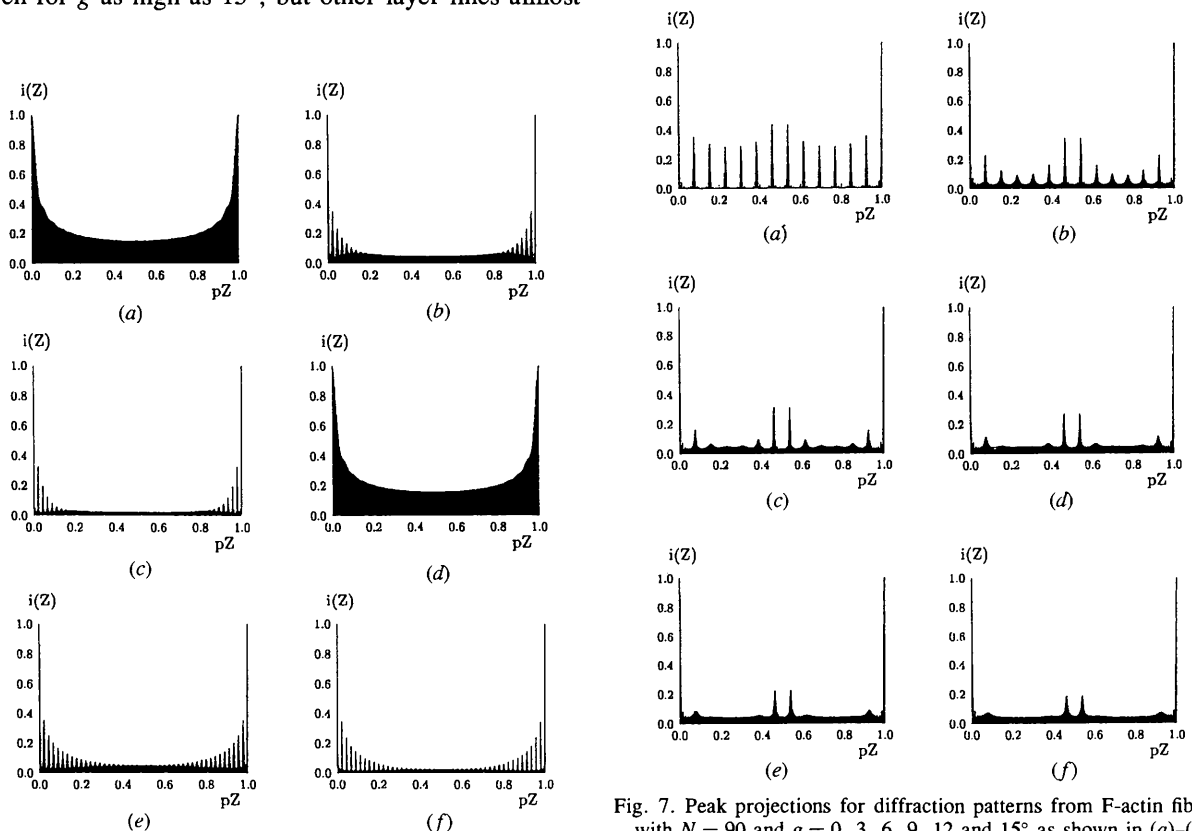


Fig. 6. Peak projections for HbS fiber with $u = 48$, $g = 2.7/360$ and (a) $N = 24$, (b) $N = 96$ and (c) $N = 192$. The projections for $g = 1.0/360$ are shown in (d), (e) and (f) for comparison, with identical values of N as in (a), (b) and (c), respectively. The summation for $i(Z_1)$ was extended from $n = -96$ to $n = 96$ in a reciprocal-space range of $Z = Z_1 - 0.5/p$ to $Z = Z_1 + 0.5/p$.

Fig. 7. Peak projections for diffraction patterns from F-actin fibers with $N = 90$ and $g = 0, 3, 6, 9, 12$ and 15° as shown in (a)–(f). The summation for the projection was extended from $n = -52$ to $n = 52$ in a reciprocal-space range of $\pm 0.5/p$. All of the layer lines, 0 to 13, can be detected in the diffraction pattern if $g \leq 3^\circ$, while the layer lines 3, 4, 9 and 10 disappear as g increases to 6° . Another two lines, 2 and 11, become undetectable when $g = 9^\circ$, and only layer lines 6 and 7, and possibly 1 and 12, appear in the pattern.

form of equation, describing the effect of disorder and helix length on any Bessel term, can be obtained and, if the layer line is dominated by a single Bessel term, this equation is a good approximation for the whole layer-line intensity.

Egelman & DeRosier (1982) started the investigation of the effects of cumulative angular disorder on X-ray diffraction from disordered fibers. They found that for long fibers the layer-line intensities reduce and broaden by a factor proportional to n^2 , the square of the related Bessel order. Barakat (1987) extended Egelman & DeRosier's result by rigorous statistical treatment so that the layer-line intensity was obtained in explicit form for disordered fibers with any length. Inouye (1994) studied layer-line-intensity distribution along the Z direction, not only the intensity maxima, and obtained an equation of the distribution for long fibers. The results we present here are extensions of the above-mentioned authors' results. We have carried out a rigorous analytical treatment of X-ray diffraction from a cumulative azimuthally disordered helix with any length and obtained an equation in explicit form, describing the Z-direction distribution of any Bessel term in the pattern. That work made possible an analysis of the reduction of peak intensity, the broadening and the overlap of layer lines in diffraction patterns from disordered helices over a very wide range of disorder degree and the helix length. The results were applied to HbS fibers where approximations made in previous treatments are not valid.

This work was supported by the National Institutes of Health, grant HL 28381, and a grant from the National Science Foundation.

References

- Barakat, R. (1987). *Acta Cryst.* **A43**, 45–49.
- Briehl, R. W., Mann, E. S. & Josephs, R. (1990). *J. Mol. Biol.* **211**, 693–698.
- Carragher, B., Bluemke, D. A., Gabriel, B., Potel, M. J. & Josephs, R. (1988). *J. Mol. Biol.* **199**, 315–331.
- Cochran, W., Crick, F. H. C. & Vand, V. (1952). *Acta Cryst.* **5**, 581–586.
- Dykes, G. W., Crepeau, R. H. & Edelstein, S. J. (1979). *J. Mol. Biol.* **130**, 451–472.
- Egelman, E. H. (1992). *Curr. Opin. Struct. Biol.* **2**, 286–292.
- Egelman, E. H. & DeRosier, D. J. (1982). *Acta Cryst.* **A38**, 796–799.
- Egelman, E. H., Francis, N. & DeRosier, D. J. (1982). *Nature (London)*, **298**, 131–135.
- Fairchild, B. M. & Chiu, C. C. (1979). *Proc. Natl Acad. Sci. USA*, **76**, 223–226.
- Franklin, R. E. & Klug, A. (1955). *Acta Cryst.* **8**, 777–780.
- Gradshteyn, I. S. & Ryzhik, I. M. (1980). *Tables of Integrals, Series and Products*, p. 31. New York: Academic Press.
- Holmes, K. C., Popp, D., Gebhard, W. & Kabsch, W. (1990). *Nature (London)*, **347**, 44–49.
- Inouye, H. (1994). *Acta Cryst.* **A50**, 644–646.
- Lewis, M. R., Gross, L. J. & Josephs, R. (1994). *Microsc. Res. Tech.* **27**, 459–467.
- Popp, D., Lednev, V. V. & Jahn, W. (1987). *J. Mol. Biol.* **197**, 679–684.
- Scherrer, P. (1918). *Nachr. Göttinger Ges.* p. 98.
- Vainstein, B. K. (1966). *Diffraction of X-ray by Chain Molecules*. Amsterdam: Elsevier.
- Watson, G. N. (1947). *Treatise on the Theory of Bessel Functions*, pp. 22, 79. Cambridge University Press.
- Worthington, C. R. & Elliot, G. F. (1989). *Acta Cryst.* **A45**, 645–654.